

Mass loss rate determination of southern OB stars

P. Benaglia^{1,*}, C. E. Cappa^{1,2,*}, and B. S. Koribalski³

¹ Instituto Argentino de Radioastronomía, C.C.5, (1894) Villa Elisa, Buenos Aires, Argentina

² Fac. de Cs. Astronómicas y Geofísicas, La Plata National University, Paseo del Bosque S/N, (1900) La Plata, Argentina

³ Australia Telescope National Facility, CSIRO, PO Box 76, Epping, NSW 1710, Australia

Received 1 March 2001 / Accepted 23 April 2001

Abstract. A sample of OB stars (eleven Of, one O and one B supergiant) has been surveyed with the Australia Telescope Compact Array at 4.8 and 8.64 GHz with a resolution of $\sim 2''$ – $4''$. Five stars were detected; three of them have negative spectral indices, consistent with non-thermal emission, and two have positive indices. The thermal radiation from HD 150135 and HD 163181 can be explained as coming from an optically thick ionized stellar wind. The non-thermal radiation from CD-47° 4551, HD 124314 and HD 150136 possibly comes from strong shocks in the wind itself and/or in the wind colliding region if the stars have a massive early-type companion. The percentage of non-thermal emitters among detected O stars has increased up to $\sim 50\%$. The Of star HD 124314 clearly shows flux density variations. Mass loss rates (or upper limits) were derived for all the observed stars and the results compared with non-radio measurements and theoretical predictions.

Key words. stars: early-type – stars: mass loss – stars: winds, outflows – radio continuum: stars

1. Introduction

Of stars are characterized by N[III] $\lambda\lambda$ 4630–34 Å emission lines and He[II] λ 4686 Å emission or absorption lines in their spectra. According to Maeder (1990) a massive O star evolves into an Of star which, in turn, goes through the blue supergiant and luminous blue variable phases, and after that becomes a Wolf Rayet (WR) star. In addition, Of stars have very strong winds with gas terminal velocities up to 3000 km s^{-1} (Chlebowski & Garmany 1991). The velocities, derived from P Cygni profiles, are appreciably larger than the stellar escape velocity, proving that important mass loss is taking place in Of stars. Typical values for the mass loss rate, \dot{M} , of Of stars are $\lesssim 10^{-5} M_{\odot} \text{ yr}^{-1}$ (Lamers et al. 1995).

Like for WR stars, the action of the wind on the ambient interstellar medium produces a cavity of hot rarefied gas surrounded by a slowly expanding envelope. The shells can be detected at optical and radio wavelengths (Lozinskaya 1982; Cappa & Benaglia 1998; Benaglia & Cappa 1999). Using high resolution, the wind region itself is observable in the radio continuum emission. The stellar mass loss rate (or an upper limit) can be estimated from the radio flux density. Accurate determinations of \dot{M} are essential in modeling the stellar evolution, describing the

Of-stellar wind and changes in the ambient gas caused by the mass outflow. Since radio-determined mass loss rates turned out to be among the most reliable ones, they are used to calibrate \dot{M} obtained with other methods, i.e. involving H α equivalent widths or UV profiles.

It is commonly assumed that the dominant driving mechanism for the winds is radiation pressure. However, \dot{M} values predicted by radiation-driven wind models differ up to a factor of two with the observed mass loss rates for O-type supergiants (Vink et al. 2000). Puls et al. (1996) found the discrepancies between observed and predicted mass loss rates diminished when considering more accurate input parameters of the involved atomic physics (see Kudritzki & Puls 2000 for a comprehensive review). In this respect, new results on \dot{M} are crucial for testing the existing wind models and theoretical predictions.

Using the Very Large Array (VLA), systematic observations of O, B and WR stars were carried out by Abbott et al. (1986) and Bieging et al. (1989), while more recently Scuderi et al. (1998) also observed Of as well as O and B-type stars. With the Australia Telescope Compact Array (ATCA¹), Leitherer et al. (1997) extended the study towards southern declinations, observing a complete sample of WR stars closer than 3 kpc. Up to now, only a few

Send offprint requests to: P. Benaglia,
 e-mail: paula@irma.iar.unlp.edu.ar

* Member of Carrera del Investigador, CONICET.

¹ The Australia Telescope is funded by the Commonwealth of Australia for operation as a National Facility managed by CSIRO.

southern OB stars were observed (e.g. Leitherer et al. 1995). We have initiated a programme with the aim of detecting bright early-type stars that remain unobserved at radio wavelengths in the southern sky. Here we present the results obtained so far, after the first two observing campaigns.

The next section gives characteristics of the selected sample of OB stars. Section 3 describes the observations and reduction procedure. The theoretical formulae used here are briefly described in Sect. 4. The results are presented in Sect. 5 and discussed in Sect. 6. We close with the conclusions in Sect. 7.

2. The target stars

From the lists published by Cruz-González et al. (1974) and Garmany et al. (1982) we selected all southern stars (declinations south of -24°), closer than 3 kpc and still unobserved at cm wavelengths. These stars form our working database.

We derived an *expected* mass loss rate with the approximation given by Lamers & Leitherer (1993). Their formula gives \dot{M} as a function of effective temperature, T_{eff} , and stellar luminosity, L_* . The values for T_{eff} and L_* were taken from Vacca et al. (1996). By means of the standard model for thermal emission from stellar winds (Wright & Barlow 1975; Panagia & Felli 1975) we computed a minimum detectable mass loss rate, assuming the radio flux as two times the predicted rms after 3 hours integration time with the ATCA. The predicted rms noise resulted in 0.050 mJy at 3 cm, and 0.054 mJy at 6 cm, if continuum emission from the target stars was not contaminated with confusion from other sources in the field. Finally, we defined an index F equal to the expected mass loss rate over the minimum detectable mass loss rate, and ranked our stars according to that index.

The present target stars were chosen from the database depending on the allocated time, and favoring the objects with highest index F , i.e. the closest and earliest. The candidates are listed in Table 1. For this sample, the minimum detectable mass loss rates were $(1-3) \times 10^{-6} M_\odot \text{ yr}^{-1}$.

We have included the already observed star HD 57060 (29 CMa), which was not detected with the VLA (Abbott et al. 1980), in the target list because, besides matching most of the criteria, it is a very interesting Of+O binary system. The rms noise expected from the ATCA, 0.050 mJy, is 8σ lower than the reported VLA flux limit of 0.4 mJy. The masses of both the primary and secondary stars are in the range 20–30 M_\odot , the primary being the more evolved star (Hutchings 1977; Stickland 1989). Wiggs & Gies (1993) interpreted the H α P Cygni profile by means of a model where emission comes from inside the wind of the primary and from a plane midway between the stars where the winds collide.

H α emission has also been reported in HD 163181 (Thaller 1997) and thus this binary star can be suspected to have colliding winds.

VLA 6-cm observations towards the field of HDE 319718 (N35 according to Neckel 1984) were presented by Felli et al. (1990). Again, using the ATCA at 3 and 6 cm we intended to obtain a more sensitive image.

Table 1 lists the stellar parameters, beginning with the name, spectral classification and photometric data. Information concerning possible membership to a stellar association is given in Col. 6. The spectro-photometric distance was estimated using the M_v and $(B - V)_0$ values from Vacca et al. (1996) and Schmidt-Kaler (1982), respectively. In the case of HD 163181, the absolute magnitude was extrapolated. In all cases but HD 101205, the distances estimated by us were, within errors, in agreement with the distances to the OB associations. We adopted as the stellar distances d the cluster distances whenever available, and the spectro-photometric distances for field stars. The mass loss rates quoted in Table 1 were derived by means of optical and UV spectra. When no measured terminal velocities (v_∞) were found in the literature, the values were interpolated from Prinja et al. (1990) and appear in brackets. Column 9 accounts for the binary status. The label “BIN” stands for the stars catalogued as binaries with computed orbits. Following Gies (1987) SB2? means that double lines have been reported, but no orbit was determined; SB1? indicates that the star is a possible spectroscopic binary; and C, that the radial velocity was taken as constant, i.e. as for single stars.

3. Observations and analysis

The observations presented here were obtained with the Australia Telescope Compact Array in two campaigns: 1) in 1998, February 16/17, using the 6A configuration, and 2) in 2000, March 30 + April 1/2, with the 6D configuration, collecting a total of 52 h observing time. In both sessions the maximum baseline was 6 km.

Each source was observed simultaneously at two frequencies: 8.64 GHz (3 cm) and 4.8 GHz (6 cm), with a total bandwidth each of 128 MHz over 32 channels. The average time on source was 2.5 to 3 h, exception made for HD 124314 which was observed on three occasions, in looking for flux variability. The stars were observed during intervals of 15 or 30 min, interleaved with short observations of close phase calibrators, and spanned over an LST range of ~ 11 hours for most of them. The allocated time allowed us to track the sources HD 57060, HD 163181 and HDE 319718 for ~ 7 h each. The flux density scale was calibrated using observations of the primary calibrator, 1934–638, assuming flux densities of 2.84 Jy at 3 cm and 5.83 Jy at 6 cm.

The data were reduced with Miriad routines and analyzed with the AIPS package. After data calibration the visibilities were Fourier-transformed using “natural-” and “uniform-” weighting. The images obtained in the former way turned out to have better signal to noise ratio. The restoring beams were $\gtrsim 1''.5$ at 3 cm and $\gtrsim 3''$ at 6 cm. In many cases, the diffuse emission from extended sources

Table 1. Stellar parameters for the target stars.

Name	Sp.Class.	m_v	$(B - V)$	d (kpc)	Assoc.	$\log(\dot{M})$ (M_\odot/yr)	v_∞ (km s^{-1})	Binary status
HD 57060	O8.5If ¹	4.90 ¹	-0.14 ¹	1.5	NGC 2362 ²	-5.64 ³	1425 ⁴ , 1800 ⁵	BIN ⁶
	O8Iaf+O ⁷					-5.07 ⁸	1700 ⁹	
CD-47° 4551	O5If ¹⁰	8.39 ¹¹	0.89 ¹¹	1.7			[1885]	
HD 94963	O6.5III(f) ¹²	7.18 ¹	-0.09 ¹	2.2	Car OB2 ²		[2545]	C ²
HD 97253	O5.5III(f) ¹²	7.12 ¹	0.15 ¹	2.2	Car OB2 ²		[2600]	BIN ²
HD 101205	O7IIIIn(f) ¹²	6.48 ¹	0.07 ¹	2.5	Cru OB1 ²		2740 ⁴	SB2? ²
HD 112244	O8.5Iab(f) ¹²	5.33 ¹	0.01 ¹	1.5		-5.30 ⁸	1950 ⁶ , 1880 ¹³	SB1? ²
							2160 ¹⁴ , 1575 ⁴	
HD 124314	O6V(n)((f)) ¹²	6.64 ¹	0.21 ¹	1.0		-5.15 ⁸	2500 ⁴	SB1? ²
HD 135240	O7.5III((f)) ¹⁵	5.08 ¹	-0.06 ¹	1.0		-6.21 ¹⁶	2460 ⁴ , 2700 ⁵	BIN ²
HD 135591	O7.5III((f)) ¹⁵	5.43 ¹	-0.09 ¹	1.2		-6.40 ⁸ , -7.26 ¹⁷	2600 ¹⁷ , 2235 ⁴	BIN ¹⁸
HD 150135	O6.5V((f)) ¹⁵	6.89 ¹	0.13 ¹	1.4	Ara OB1a ²		[2455]	SB1? ^{2,6}
HD 150136	O5IIIIn(f) ¹⁵	5.64 ¹	0.14 ¹	1.4	Ara OB1a ²		3160 ⁴	BIN ⁶
HD 163181	B1Iape ¹⁰	6.43 ¹⁹	0.52 ¹⁹	1.4		-5.15 ⁸	520 ⁴	BIN ²⁰
	BN0.5Iap ²¹							
HDE 319718	O7III ²² , O3III ¹³	10.43 ²²	1.48 ²²	1.7	NGC 6357 ^{23,24}		[2295]	

1 – Cruz-González et al. (1974); 2 – Gies (1987); 3 – Drechsel et al. (1980); 4 – Howarth et al. (1997); 5 – Hutchings & von Rudloff (1980); 6 – Chlebowski & Garmany (1991); 7 – Garmany, Conti & Massey (1980); 8 – Hutchings (1977); 9 – Hutchings (1976); 10 – Garrison et al. (1977); 11 – Drilling (1991); 12 – Walborn (1973); 13 – Vijapurkar & Drilling (1993); 14 – Bernabeu et al. (1989); 15 – Walborn (1972a); 16 – Prinja & Howarth (1986); 17 – Conti & Garmany (1980); 18 – Lindroos (1985); 19 – Garmany, Conti & Chiosi (1982); 20 – Levato et al. (1988); 21 – Walborn (1972b); 22 – Neckel (1984); 23 – Johnson (1973); 24 – Felli et al. (1990).

towards the observed fields had to be removed by taking out the visibilities corresponding to the shortest baselines.

Flux density values of the thirteen observed sources are listed in Tables 2a and 2b. The three entries of HD 124314 correspond to the different observing dates (C1: Campaign 1, and C2: Campaign 2). The optical positions were taken from the SIMBAD database. Four sources were detected at both frequencies, with flux densities greater than 3σ . HD 150135 was detected at 3 cm only; at 6 cm it appears at a 2.5σ level. All detected sources were unresolved: CD-47° 4551, HD 124314, HD 150135, HD 150136 and HD 163181. Bi-dimensional Gaussians were fitted to the five sources using Miriad task *Imfit*, and the positions of the maxima are given as the radio position in Table 2a. The differences with optical coordinates, whenever present, are $\leq 0''.5$, so the optical and radio positions are in good agreement within the errors. The flux density was computed after correcting the zero level in the images. The flux density error in the Tables is equal to the image rms noise (σ). For the undetected stars, a maximum flux density of 3σ is quoted. The integration time on source is listed in Tables 2a and 2b as t_{int} .

Figures 1 to 4 display the detected stars, at 3 and 6 cm. The restoring beam is plotted in each case.

4. Radio emission from stellar winds

Stars with ionized winds show a flux density excess towards long wavelengths. Assuming the continuum radiation is due to free-free emission (thermal bremsstrahlung),

Wright & Barlow (1975) and Panagia & Felli (1975) deduced the spectrum in the radio and IR energy ranges. Their model was developed for a uniform flow expanding at constant velocity, and allows to derive the stellar mass loss rate as a function of the measured flux density as:

$$\dot{M} = 5.32 \times 10^{-4} \frac{S_\nu^{3/4} d^{3/2} v_\infty \mu}{Z \sqrt{\gamma} g_\nu \nu} M_\odot \text{ yr}^{-1}. \quad (1)$$

Here d is the stellar distance in kpc, v_∞ the wind terminal velocity in km s^{-1} , S_ν the flux density in mJy; μ stands for the mean molecular weight, γ is the mean number of electrons per ion and Z , the rms ionic charge.

In the range of the wind electron temperatures T_e and observing frequencies we are dealing with, the free-free Gaunt factor can be approximated by:

$$g_\nu = 9.77 \left(1 + 0.13 \log \frac{T_e^{3/2}}{Z\nu} \right).$$

The model predicts a spectral index $\alpha = 0.6$ ($S_\nu \propto \nu^\alpha$) in accordance with measurements of various WR and O stars. If the spectral index differs from 0.6, Eq. (1) yields an upper limit to the stellar mass loss rate. However, when detected at two or more radio continuum frequencies, an important number of stars show spectral indices approaching zero and even negative values. The interpretation of these results is consistent with a picture where the observed flux density has an important non-thermal contribution. The main non-thermal process which is relevant

Table 2a. Positions and flux densities of the detected stars.

Star	Optical RA(2000)	positions Dec.(2000)	Radio RA(2000)	positions Dec.(2000)	t_{int} (min)	$S_{3 \text{ cm}}$ (mJy)	$S_{6 \text{ cm}}$ (mJy)
CD-47° 4551	08 57 54.62	-47 44 15.7	08 57 54.61	-47 44 15.7	160	1.77 ± 0.05	2.98 ± 0.05
HD 124314	14 15 01.61	-61 42 24.4	14 15 01.61	-61 42 24.2			
C1: 02/16/1998					150	1.88 ± 0.05	2.72 ± 0.08
C2: 03/30/2000					195	2.71 ± 0.08	4.50 ± 0.07
C2: 04/02/2000					130	2.88 ± 0.05	3.78 ± 0.05
HD 150135	16 41 19.45	-48 45 47.6	16 41 19.45	-48 45 47.8	185	0.28 ± 0.03	0.10 ± 0.04
HD 150136	16 41 20.41	-48 45 46.6	16 41 20.42	-48 45 46.8	185	2.61 ± 0.03	5.57 ± 0.03
HD 163181	17 56 16.08	-32 28 30.0	17 56 16.07	-32 28 29.5	135	0.44 ± 0.05	0.20 ± 0.05

Table 2b. Flux density limits of the undetected stars.

Star	Optical RA(2000)	positions Dec.(2000)	t_{int} (min)	$S_{3 \text{ cm}}$ (mJy)	$S_{6 \text{ cm}}$ (mJy)
HD 57060	07 18 40.38	-24 33 31.3	180	<0.15	<0.15
HD 94963	10 56 35.79	-61 42 32.4	140	<0.14	<0.17
HD 97253	11 10 42.02	-60 23 04.3	140	<0.15	<0.15
HD 101205	11 38 20.36	-63 22 21.9	145	<0.13	<0.20
HD 112244	15 55 57.13	-56 50 08.9	140	<0.13	<0.15
HD 135240	15 16 56.90	-60 57 26.1	170	<0.13	<0.16
HD 135591	15 18 49.14	-60 29 46.8	180	<0.15	<0.15
HDE 319718	17 24 42.90	-34 11 48.0	180	<0.15	<0.40

for early type stars is synchrotron radiation by relativistic electrons, accelerated by first order Fermi mechanism at strong shock fronts. The presence of non-thermal radio emission provides indirect evidence for the presence of magnetic fields. In some binary stellar systems the electrons seem to be accelerated at the wind collision region (i.e. Cyg OB2 No. 5 and WR 140, Contreras et al. 1997, 1996). Eichler & Usov (1993) have shown that stellar winds collision in early type binaries may be strong sources of non-thermal radio and γ -ray emission (see also Benaglia et al. 2001 for an updated discussion).

For single stars, White (1985) has shown that electrons can be accelerated up to relativistic energies at the multiple shocks formed at the base of the wind by line-driven instabilities. The derived radio spectrum follows an index of ~ 0.5 up to a turnover around a few GHz. The relativistic electron population would generate inverse-Compton γ -rays too. Benaglia et al. (2001) have estimated the expected γ -ray luminosity from the wind colliding region, the terminal shock of the wind and the zone of the base of the wind, for Cyg OB2 No. 5, using the radio results of Contreras et al. (1997).

An interesting feature seen in some non-thermal sources is their variations in radio luminosity with time. Abbott et al. (1984) found this behaviour in 9 Sgr and

Table 3. Spectral indices of the detected stars.

Star	Spectral index $\alpha_{3-6 \text{ cm}}$
CD-47° 4551	-0.89 ± 0.06
HD 124314	
C1: 02/16/1998	-0.60 ± 0.07
C2: 03/30/2000	-0.87 ± 0.06
C2: 04/02/2000	-0.46 ± 0.04
HD 150135	$+1.75 \pm 0.70$
HD 150136	-1.29 ± 0.03
HD 163181	$+1.34 \pm 0.47$

Cyg OB2 No.9. Cyg OB2 No.5 has been extensively monitored, since ~ 1980 (see Contreras et al. 1997 and references therein). The radio source seems to switch between states of high and low emission with a period of 7 years.

5. Results

We detected five stars out of thirteen: CD-47° 4551, HD 124314, HD 150135, HD 150136 and HD 163181. Table 3 presents the spectral indices. The radio emission of the candidates CD-47° 4551, HD 124314 and HD 150136 is

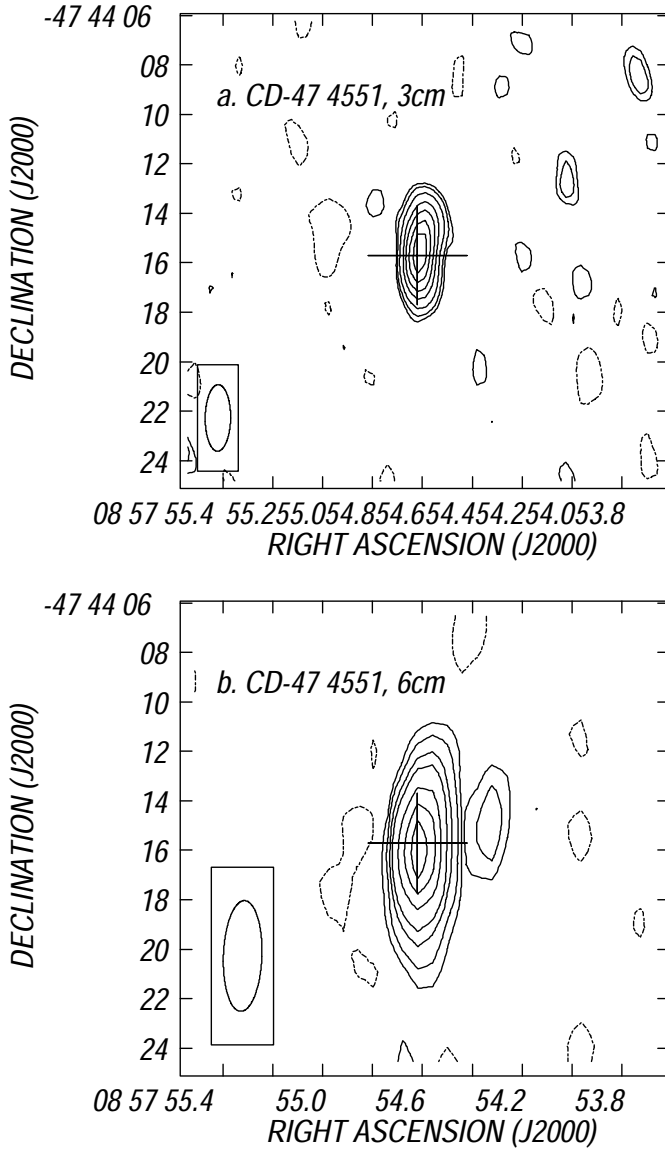


Fig. 1. a) Contour map of CD-47° 4551 at 3 cm. Contour levels are $-0.1, 0.12(2.5\sigma), 0.18, 0.3, 0.5, 0.7, 0.95$ and 1.2 mJy per beam area. The restoring beam, plotted at the bottom left corner, is 2.7×1.0 arcsec in PA -2° . **b)** The same as **a)**, at 6 cm. Contour levels are $-0.1, 0.18(3.5\sigma), 0.3, 0.5, 0.7, 1.2, 1.7$ and 2.2 mJy per beam area. The restoring beam is 4.5×1.6 arcsec in PA -2° . Negative contours are dashed. The optical position of the star is marked by a cross.

characterized by a negative spectral index between 4800 and 8640 MHz. The one of HD 124314 displays strong variations. The flux densities of these stars seem arising mainly of a non-thermal process. The only B star in the group, HD 163181, and HD 150135 show positive spectral indices, possibly indicating thermal emission as dominant.

From hereafter we shall call “thermal” sources the ones with positive spectral index, and “non-thermal” if the index is negative.

The measured flux densities at 3 cm were used to derive the mass loss rates of all target stars, because of their smaller errors compared to the flux densities at 6 cm.

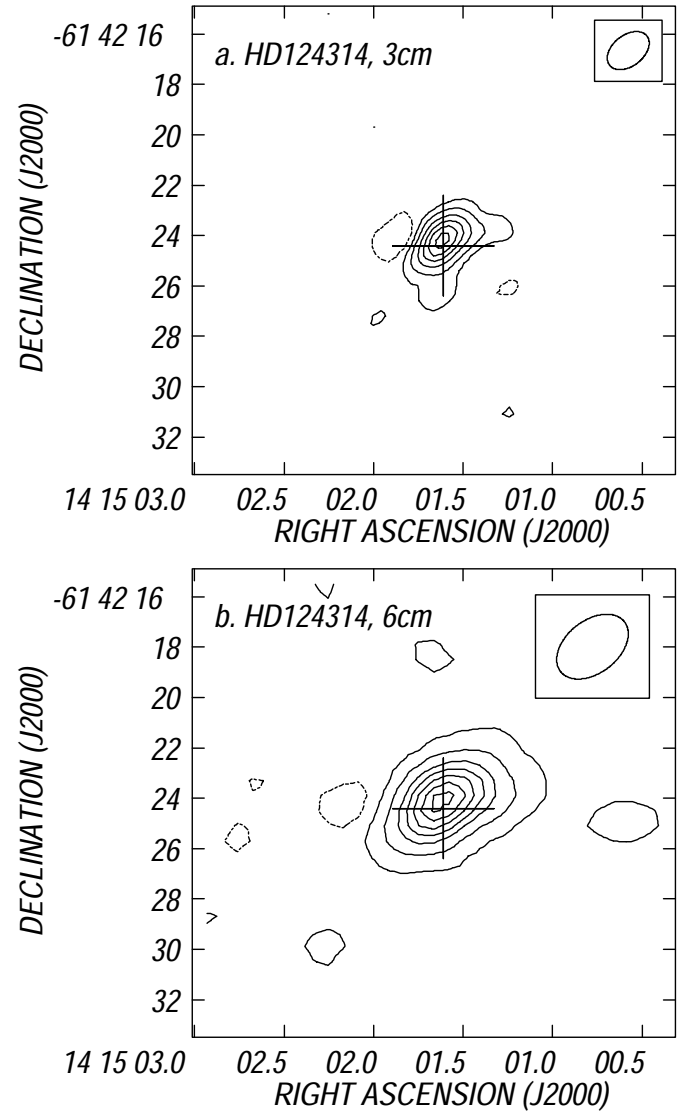


Fig. 2. a) Contour map of HD 124314 at 3 cm. Contour levels are $-0.15, 0.15(3\sigma), 0.5, 1.0, 1.5, 2.0$ and 2.5 mJy per beam area. The restoring beam, plotted at the upper right corner, is 1.9×1.2 arcsec in PA -52° . **b)** The same as **a)** at 6 cm. Contour levels are $-0.15, 0.15(3\sigma), 0.6, 1.2, 1.7, 2.2, 2.7$ and 3.2 mJy per beam area. The restoring beam is 3.2×2.1 arcsec in PA -52° .

According to their evolutionary status, for most of the target O-type stars the computed mean molecular weight was 1.5. We adopted a value of 1.3 for HD 124314 and HD 150135, the less evolved stars, and 1.6 for the only B-type star in the group. In deriving the rms ionic charge and the mean number of electrons per ion we assumed that both hydrogen and helium were singly ionized, and that in the region where the radio emission comes from, the He^{++} had the chance to recombine. The electron temperature was assumed as 0.4 the effective stellar temperature. The computed values of μ , Z , and γ are listed in Table 4, together with the free-free Gaunt factor at 3 cm.

We derived the mass loss rates by means of Eq. (1), independently of the behaviour of the flux density with

Table 4. Radio-derived mass loss rates.

Star	T_e (K)	μ	Z	γ	$g_{3\text{ cm}}$	$\log(\dot{M})$ (M_\odot/yr)
HD 57060	14 300	1.5	1.0	1.0	5.1	< -5.52
CD-47° 4551	17 900	1.5	1.0	1.0	5.3	(-4.62)
HD 94963	16 500	1.5	1.0	1.0	5.2	< -5.15
HD 97253	17 600	1.5	1.0	1.0	5.2	< -5.11
HD 101205	16 000	1.5	1.0	1.0	5.2	< -5.08
HD 112244	13 700	1.5	1.0	1.0	5.0	< -5.54
HD 124314	17 400	1.3	1.0	1.0	5.2	(-4.74)
HD 135240	15 400	1.5	1.0	1.0	5.1	< -5.69
HD 135591	15 400	1.5	1.0	1.0	5.1	< -5.49
HD 150135	16 900	1.5	1.0	1.0	5.2	-5.23
HD 150136	18 200	1.5	1.0	1.0	5.3	(-4.40)
HD 163181	11 600	1.6	0.9	0.8	5.0	-5.63
HDE 319718	15 900	1.5	1.0	1.0	5.2	< -5.34

frequency (see Table 4). The results for candidates with spectral index $\alpha < 0$ appear in parenthesis. For non-detections and non-thermal sources, the derived mass loss rates must be considered as upper limits.

In the computation of the mass loss rate errors we have adopted the relative deviations for μ , γ , g_ν and Z of $\sim 10\%$, and for the terminal velocity an accuracy better than 20% . The flux density errors contribute with $\sim 10\%$ in the worst cases. Undoubtedly the main source of error in \dot{M} is the uncertainty in stellar distances. If the relative error is of 20% , the resulting $\sigma(\log(\dot{M})) \approx 0.2$. This last value increases to 0.3 in the more conservative case of distances accurate up to 30% .

Inhomogeneities or anisotropy in the winds like clumpiness or collimated flows are other causes of errors in \dot{M} when estimated from the model of Wright & Barlow (1975).

Among the eight non-detected stars, five had predicted mass loss rates of the order of the minimum detectable mass loss rates, and we expected that they would be detected at a 2σ level. The stars HD 57060 and HD 112244 have both expected mass loss rates, and mass loss rates derived by optical means appreciably larger than the minimum detectable mass loss rates.

5.1. Comments on individual stars

HD 57060. This source was observed for 3 hours with the ATCA and was not detected. The rms of the final images agrees with the expected rms of 0.05 mJy at 3 cm, and 0.054 mJy at 6 cm. According to these values we conclude that the flux density of this star must be below 0.15 mJy, and the mass loss rate less than $3 \times 10^{-6} M_\odot \text{ yr}^{-1}$. Abbott et al. (1980) reported no detection at 6 cm above 0.4 mJy after 165 min of integration time with the VLA.

CD-47° 4551. Besides the target star, at 4800 MHz a second source appears $5.4''$ to the west, with a maximum over 6σ (Fig. 1b). Its flux density is 0.33 mJy at 6 cm. The non detection of this small source at 3 cm means that the

flux density is $S_{3\text{ cm}} < 0.15$ mJy, letting us to conclude that the spectral index is negative. At 1.7 kpc the spatial distance between the two maxima is about 9000 AU.

HD 94963, HD 97253, HD 101205, HD 112244, HD 135240 and HD 135591. The observations allowed us to estimate upper limits to mass loss rates for these undetected stars.

HD 124314. This star was first detected on February 1998. The measured flux densities at 3 and 6 cm yield a non-thermal spectral index of -0.60 . Figure 2 depicts the stellar wind as observed the first day of C2. In order to look for variability with timescales of years and days, we reobserved the source on March 30 and April 2, 2000.

For this particular star we produced, at each frequency, three images, maintaining the number of iterations, the baselines (greater than 10 k λ) and the restoring beams ($2''$ at 3 cm and $3.6''$ at 6 cm). Although we were not able to appreciate differences in shape between the maps made using data taken at different dates, the observed flux densities showed large variations (see Table 2a).

At 3 cm the variability is appreciable between observations of 1998 and 2000, as an increase of $\sim 50\%$. Flux densities of C2 did not present differences within the error.

The source displayed always variations when observed at 6 cm. The flux densities measured at 2000 are 65% and 40% greater than the corresponding one of 1998. During the three days-interval of C2 the flux decreased about 15% .

The mass loss rate of HD 124314 was derived from the observations with the highest spectral index, i.e., for which the non-thermal contribution to the flux densities were the smallest.

HD 150135 and HD 150136. Figure 3 displays the radio images of these two stars. HD 150135 is barely detected at 6 cm, with $S_{6\text{ cm}} \approx 2.5\sigma$. The earliest and strongest source, HD 150136, has a singular shape. Although elongated as the observing beam, it shows extensions to both sides, visible at the two observing frequencies.

HD 163181. At 6 cm it is a 4σ detection, being the flux density about half of that at 3 cm (see Fig. 4 and Table 2b).

HDE 319718. This star is located near the H II region G353.2+0.9. The 6 -cm VLA map of the ionized gas (Felli et al. 1990) has a peak of ~ 120 mJy, and covers a region of $2'$ in diameter, $1'$ north of our target star. To eliminate completely the emission from the extended sources, the ATCA image was built considering visibilities of baselines only with antenna 6. The candidate was undetected above 0.15 mJy at 3 cm. However, upper limits to the flux density permitted us to derive a corresponding limit to the mass loss rate.

5.2. Other sources in the fields

Towards the direction of the target stars two previously unknown sources were detected, named S1 and S2. They

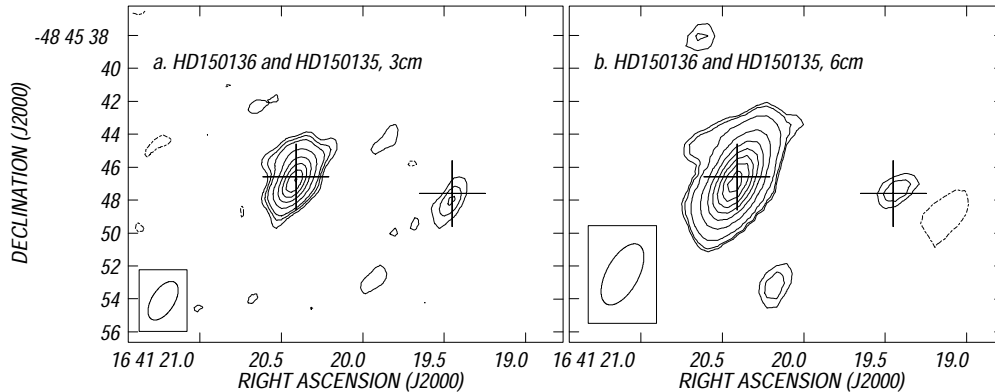


Fig. 3. **a)** Contour map of HD 150135 and HD 150136 at 3 cm. Contour levels are $-0.08, 0.12(4\sigma), 0.2, 0.3, 0.6, 1.0, 1.4, 1.8$ and 2.2 mJy per beam area. The restoring beam, plotted at the bottom left corner, is 2.6×1.4 arcsec in PA -33° . **b)** The same as a) at 6 cm. Contour levels are $-0.15, 0.15(5\sigma), 0.2, 0.4, 1.0, 1.75, 2.5, 3.25, 4.0$ and 4.75 mJy per beam area. The restoring beam is 4.1×2.0 arcsec in PA -33° .

are visible at the two observed frequencies and are point sources for ATCA.

S1 is located in the field of HD 94963, at the radio position $\alpha = 10^{\text{h}}56^{\text{m}}29.27^{\text{s}}, \delta = -61^\circ43'1.19''$. The measured flux densities are $S_{3\text{ cm}} = 3.8 \pm 0.05$ mJy and $S_{6\text{ cm}} = 6.4 \pm 0.06$ mJy, thus the spectral index results in -1.16 .

The second source is located at $\alpha = 15^{\text{h}}18^{\text{m}}35.49^{\text{s}}, \delta = -60^\circ29'59.44''$ in the field of HD 135591. Its radio flux densities are $S_{3\text{ cm}} = 0.24 \pm 0.05$ mJy and $S_{6\text{ cm}} = 0.60 \pm 0.05$ mJy, giving a spectral index of -0.68 .

Possible counterparts to these objects were searched using NED and SIMBAD databases and SkyView² images from the Digitized Sky Survey³ (DSS), with no positive results. The radio negative spectral indices indicate a non-thermal origin of the emission. This fact, together with the small angular size of the sources and the non existence of other related object suggest an extragalactic origin for S1 and S2.

6. Discussion

6.1. Statistics on OB radio observations

In order to perform some statistics on radio detections of OB stars, we have consulted the articles of Abbott et al. (1980, 1981, 1984), Bieging et al. (1989), Leitherer et al. (1995), Contreras et al. (1996), Waldron et al. (1998) and Scuderi et al. (1998), and added the results of this work. Regarding these investigations, about 120 OB stars have been observed, and less than 40 detected at least at one frequency.

² SkyView was developed under NASA ADP Grant NAS5-32068 with Principal Investigator Thomas A. McGlynn under the auspices of the High Energy Astrophysics Science Archive Research Center (HEASARC) at the GSFC Laboratory for High Energy Astrophysics.

³ The Digitized Sky Survey was produced at the Space Telescope Science Institute under US Government grant NAG W-2166.

Excluding our observations, about 25 stars were detected at two or more frequencies, allowing the determination of spectral indices. Of the almost 40 detected sources, $\sim 50\%$ classify as thermal, $\sim 25\%$ as non-thermal, and $\sim 25\%$ as composite or undecided.

No non-thermal B stars were found, giving support to the suggestion of Bieging et al. (1989) that the synchrotron mechanism is less efficient at lower luminosities.

After the detections presented here the thermal candidates stay around 50% between the detected O and B-type stars, while the non-thermal ones have increased from 25% to 30%. For detected O-type stars, the figures are more striking: the thermal candidates are $\sim 40\%$ (before and after this work), but the percentage of non-thermal O stars changes from 40% to almost 50% after the present results. Chapman et al. (1999) arrived at a similar result for WR stars, in surveying all candidates at negative declinations and distances less than 3 kpc. We think that the number of non-thermal candidates must be taken as a lower limit because:

- i) a single O star with powerful winds can radiate non-thermal radio emission due to relativistic leptons. According to the model of White (1985), a spectral index of $+0.5$ will be measured at low frequencies, mimicking a thermal spectrum;
- ii) the flux density of a non-thermal source is known to vary, and at the time of the observation a minimum can be occurring, approaching a thermal spectrum.

6.2. Flux variability and HD 124314

It is important to analyze the variations of the flux density in HD 124314. They could be originated in changes in the mass loss rate, ionization or density structure that take place throughout the photosphere of the star. The corresponding time scale depends on the observing frequency. Scuderi et al. (1998) and Waldron et al. (1998) give expressions to estimate the time scales of the variations.

Let R_{eff} be the characteristic radius of the emitting region, given by Wright & Barlow (1975) for a thermal

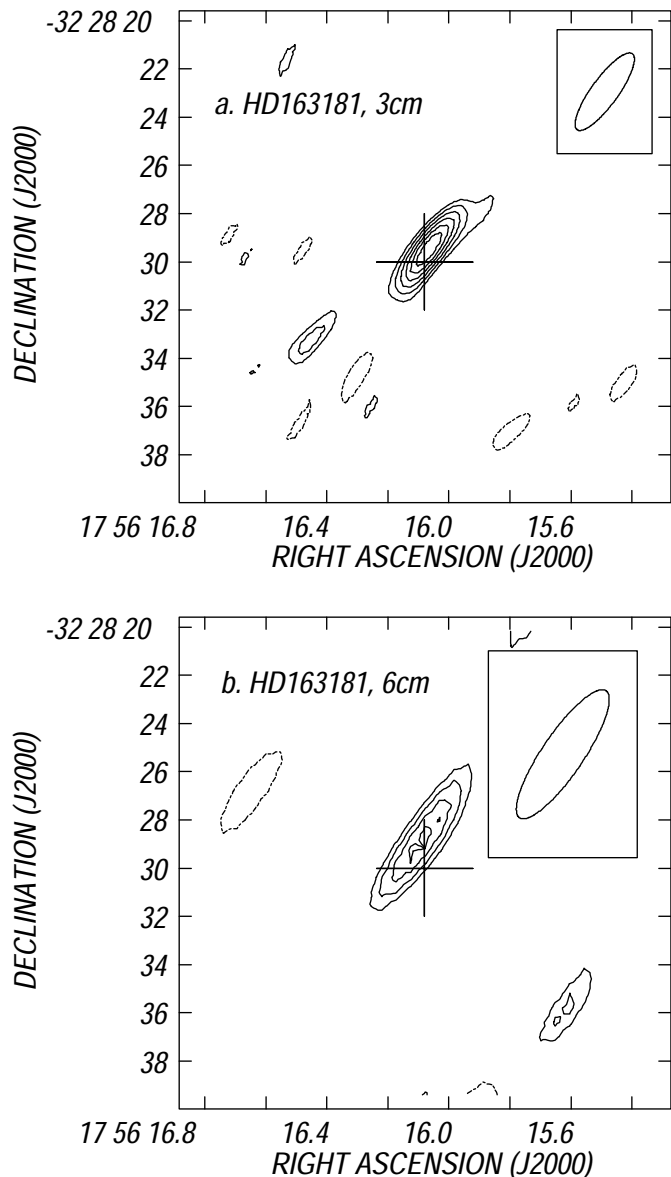


Fig. 4. **a)** Contour map of HD 163181 at 3 cm. Contour levels are $-0.15, 0.15(3\sigma), 0.2, 0.25, 0.3, 0.35$ and 0.4 mJy per beam area. The restoring beam, plotted at the upper right corner, is 3.9×1.1 arcsec in PA -34° . **b)** The same as **a)** at 6 cm. Contour levels are $-0.13, 0.13(2.5\sigma), 0.17, 0.21$ and 0.25 mJy per beam area. The restoring beam is 6.4×1.7 arcsec in PA -34° .

outflow. When considering the mass loss rate predicted using Vink et al. (2000) models for HD 124314, $R_{\text{eff}} \approx 1200 R_\odot$ and the transit time of the shock front in the radio regime will be >5 days for variations in \dot{M} . On the other hand, variations in ionization are characterized by time scales of ≥ 20 days in the radio emission. The flux density changes must be faster towards higher frequencies, as R_{eff} diminishes.

Following the model of Waldron et al. (1998), the time travel for a density disturbance to propagate from the X-ray radius to the radio radius is above 10 days.

Taking the above considerations into account, is clear that the flux variation between C1 and C2 can be

ascribed to the mentioned phenomena. In contrast, it seems difficult to find the same causes for the differences between the flux densities of the two observing runs during C2, which are separated just three days and occur at 6 cm but not at 3 cm. A simpler explanation is to assume that the quoted flux density errors are underestimated. Nonetheless, it will be interesting to perform a series of observations with time scales of a few days towards this star, which is proposed as a counterpart to the unidentified gamma-ray source 3EG J1410-6147 (Romero et al. 1999).

6.3. Comparison between radio-derived \dot{M} and other estimates

The mass loss rates derived here were compared to observed values found in the literature and from the new models of Vink et al. (2000). For the target stars, previous estimates of \dot{M} were derived from optical and UV profiles. The theoretical -expected- mass loss rates can be computed from Vink et al.'s models, as a function of the effective temperature, luminosity, mass, and wind terminal velocity. For our calculations we have adopted the stellar parameters given by Vacca et al. (1996). One must bear in mind that predicted values were calculated with parameters derived under a series of assumptions from models, depending on a certain spectral classification, which is not unique.

Table 5 lists the mass loss rates obtained from the literature, Vink et al., and us. For the correlation we have assumed error bars of $\sim 50\%$ \dot{M} in the values derived in this work.

The result of the comparison showed no pattern. For the stars HD 94963, HD 97253, HD 101205, HD 135591 and HDE 319718 the predicted and the radio values are in good agreement (see Cols. 3 and 4 of Table 5), although we would have expected radio signal around a 2σ level for most of them.

Despite HD 57060 spectral classification (Of+O), its predicted and optically derived mass loss rate, it was not detected at 3 or 6 cm. Using Eq. (1), we computed an expected flux density, S_ν^* , if $\dot{M} = \dot{M}_{\text{optical}} = 8.51 \times 10^{-6} M_\odot \text{ yr}^{-1}$. We found $S_{3 \text{ cm}}^* \approx 0.6 \text{ mJy} > 4S_{3 \text{ cm}}$ and $S_{6 \text{ cm}}^* \approx 0.4 \text{ mJy} > 2S_{6 \text{ cm}}$. The same relation of predicted and optically derived with radio mass loss rate happens to HD 112244. Here $S_{3 \text{ cm}}^* \approx 0.27 \text{ mJy} > 2S_{3 \text{ cm}}$.

It is difficult to believe that the discrepancies between mass loss rates showed above might arise from underestimates in stellar distances, values which are, for both stars, widely accepted. Uncertainties in the wind terminal velocities are evident from Table 1. Different methods of determining v_∞ yield to a range of values: $\sim 1400\text{--}1800 \text{ km s}^{-1}$ for HD 57060, and $\sim 1600\text{--}2200 \text{ km s}^{-1}$ for HD 112244. In our calculations we have adopted $v_\infty(\text{HD 57060}) = 1800 \text{ km s}^{-1}$ and $v_\infty(\text{HD 112244}) = 1900 \text{ km s}^{-1}$. But the error on v_∞ does not suffice to account for the non-detections at radio continuum. We speculate that the

Table 5. Non-radio (n-r), predicted (VKL), and radio-derived mass loss rates.

Star	\dot{M} (n-r) (M_{\odot}/yr)	\dot{M} (VKL) ¹ (M_{\odot}/yr)	\dot{M} (radio) (M_{\odot}/yr)
HD 57060	8.51×10^{-6} 2.29×10^{-6}	7.85×10^{-6}	$<3.03 \times 10^{-6}$
CD-47° 4551		1.81×10^{-5}	2.39×10^{-5}
HD 94963		3.34×10^{-6}	$<7.16 \times 10^{-6}$
HD 97253		5.22×10^{-6}	$<7.70 \times 10^{-6}$
HD 101205		2.51×10^{-6}	$<8.38 \times 10^{-6}$
HD 112244	5.01×10^{-6}	4.06×10^{-6}	$<2.87 \times 10^{-6}$
HD 124314	7.08×10^{-6}	1.91×10^{-6}	1.81×10^{-5}
HD 135240	6.17×10^{-7}	2.02×10^{-6}	$<2.03 \times 10^{-6}$
HD 135591	3.98×10^{-7} 5.50×10^{-8}	1.81×10^{-6}	$<3.25 \times 10^{-6}$
HD 150135		1.43×10^{-6}	5.89×10^{-6}
HD 150136		5.07×10^{-6}	4.01×10^{-5}
HD 163181	7.08×10^{-6}	6.32×10^{-6}	2.37×10^{-6}
HDE 319718		2.90×10^{-6}	$<4.62 \times 10^{-6}$

1: Computed from Vink et al. (2000).

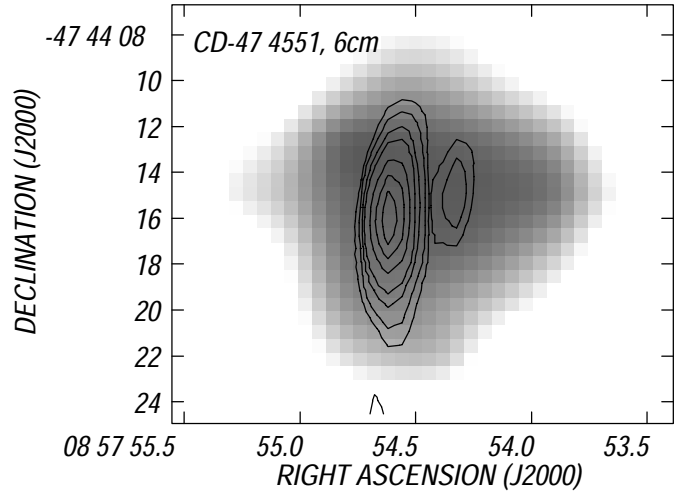
presence of variability in the mass loss rates might be an explanation. Other possibility is that some of the assumptions undertaken in deriving \dot{M} from optical lines (plus some theoretical modeling) (Hutchings 1976) are not entirely valid.

For HD 135240, probably the expected mass loss rate computed using Vink et al. (2000) formulae is an overestimation. The radio upper limit is consistent with the mass loss rate from Hutchings (1976).

The stars CD-47° 4551, HD 124314 and HD 150136, with negative spectral indices, have theoretical mass loss rates lower than the values obtained from the radio observations, as expected. The negative spectral indices are clear evidence of synchrotron contamination at 3 and 6 cm, besides the free-free contribution. This contamination may lead to the extreme case of an overestimation in \dot{M} of about an order of magnitude for HD 124314 and HD 150136, as Contreras et al. (1996) found for Cyg OB2 No. 9. The mass loss rate determined by Hutchings (1976) is similar to the radio one.

In the case of HD 150135, ($\alpha > 0$), the \dot{M} derived here resulted greater than the predicted one, as for the stars with negative spectral index. In the model of White (1985) non-thermal emission is capable of producing a spectrum with $\alpha \sim 0.5$. The search for variability can help to discriminate between a thermal or non-thermal emission mechanism.

Bieging et al. (1989) reported that the observed mass loss rates were less than predicted for B supergiants of high luminosity. They pointed out that one source of error was that the model used to compute the expected rates neglected multiply scattered photons. Notwithstanding the model of Vink et al. (2000) to derive \dot{M} takes into account scattered photons, the radio-derived mass loss rate of HD 163181 is less than predicted in a factor of 2.

**Fig. 5.** Contour map of CD-47° 4551 at 6 cm superposed on the *J*-band DSS image.

6.4. Origin of the non-thermal emission

Regarding the non-thermal sources detected here, possible origins of the emission are accretion of matter onto compact companions, shocks produced from line driven instabilities closer to the base of the wind, and in massive binary systems, at the wind collision region. Garmany et al. (1980) have estimated that at most 6% of all O stars could have an (optically) undetected companion. Bieging et al. (1989) established that systems formed by an OB star and a compact companion comprises less than 1% of all luminous OB stars. Being the frequency of compact companions so low for early-type stars, the possibility of detecting emission from this scenario becomes rather small.

HD 150136 is a known binary star and HD 124314, a possible spectroscopic binary (see Table 1 for references). The determination of the spectral classification of the secondary stars by means of optical observations is crucial to decide whether the non-thermal nature of these two candidates resides on colliding winds.

CD-47° 4551 is not recognized either as a binary or multiple star but its radio image at 4.8 GHz exhibits a second source. The *J*-band image from DSS (see Fig. 5) shows that a second optical object could be present in the direction of this candidate. There exists the possibility that the weak radio source be originated by the presence of a companion of CD-47° 4551, separated ~ 9000 AU. A possible scenario could be the following: the strongest non-thermal source, positionally coincident with the star CD-47° 4551 could be generated by inner shocks in the wind of the Of star or shocks at wind collision region if the star has a close early-type companion. The second (and also non-thermal) source could be emission from a colliding winds region between the winds of CD-47° 4551 and a visual or wide-orbit object.

The proposal stated by Chapman et al. (1999) and Dougherty & Williams (2000) that non-thermal emission could generally indicate wind interaction between a WR

and a companion gives support to the idea of the existence of a windy companion for the present non-thermal sources, as Of stars are WR precursors. Optical studies of CD-47° 4551 would be a fundamental tool to investigate its binary status.

Unfortunately, the angular resolution of the current observations does not suffice to discriminate if the non-thermal emission comes from the wind of a star or from the site where two winds collide. This kind of investigations must be carried out with very high angular resolution telescopes, like MERLIN (see for example the results of Dougherty et al. 2000 related to WR 146) and they are limited by the source declination. In addition, variability studies would bring some information to help addressing this question, in the sense that if changes in the flux density are present, the existence of an early type companion, and a wind-wind interaction region, is the most plausible explanation for the observed non-thermal radio continuum emission.

7. Conclusions

A number of conclusions can be drawn from the present observations:

- Five out of thirteen OB stars were detected at 3 and 6 cm wavelengths. The three brightest stars, CD-47° 4551, HD 124314 and HD 150136, yielded negative spectral indices, giving $\langle \alpha \rangle \approx -0.8$, whereas HD 150135 and HD 163181 gave positive spectral indices, $\langle \alpha \rangle \approx +1.5$;
- None of the target stars, except HD 57060, had previously been observed. This star presents now new (and lower) upper limits for the flux density (<0.15 mJy at 3 cm) and for the mass loss rate ($<3 \times 10^{-6} M_{\odot} \text{ yr}^{-1}$). A previous value of \dot{M} , derived from optical data was $8.5 \times 10^{-6} M_{\odot} \text{ yr}^{-1}$, and would correspond to a flux density of about 0.6 mJy at 3 cm. Variations (a decrease in this particular case) of the mass loss rate could explain the non detection above 0.15 mJy;
- More than half of the detected stars show spectral indices consistent with contamination of non-thermal emission. If many surveys of continuum emission are taken into account, the results presented here increase the percentage of non-thermal stars up to 50% among detected O-type stars. Non-thermal centimeter radio emission may be a common phenomenon in Of stars. A similar conclusion was reached by Chapman et al. (1999) concerning WR stars. These authors state that the emission would come in most cases from colliding winds;
- Either shocks in the wind if the star has no early-type companion, or shocks in the region where winds collide can explain the non-thermal emission from three target sources. The stars could have a massive companion: HD 150136 is a binary star, HD 124314 is a suspected binary, and CD-47° 4551 presents both in radio and optical wavelengths a second source separated $5''$;

- The flux density of HD 124314 was found to vary substantially. Within two years, the source almost doubled its flux;
- In this small sample, no clear correlation between detectability and distance, or spectral type, or luminosity class was found. However, the detected stars were the most luminous, early-type and closest candidates;
- The theoretical predictions recently published by Vink et al. (2000) are considered a useful tool to estimate mass loss rates, and can also help to foresee in a general way which stars are more likely to be detected. Their predictions are in general agreement with the results presented here for undetected and thermal sources.

Acknowledgements. We are in debt to the referee, Dr. C. Leitherer, for valuable comments. P.B. is grateful to the ATNF staff at Sydney and Narrabri and wishes to thank Dr. G. E. Romero for useful discussions, M. Johnston-Hollitt and R. Wark for assistance during observations and FCAG and UNLP for travel support. We acknowledge F. Bareilles, and Dr. G. Bosch for his help with web images. This work has made use of the SIMBAD database operated at CDS, Strasbourg, France, and was partially supported by CONICET (under grant PIP 607/98).

References

- Abbott, D. C., Torres, A. V., Biegging, J. H., & Churchwell, E. 1980, *ApJ*, 238, 196
- Abbott, D. C., Biegging, J. H., & Churchwell, E. 1981, *ApJ*, 250, 645
- Abbott, D. C., Biegging, J. H., & Churchwell, E. 1984, *ApJ*, 280, 671
- Abbott, D. C., Biegging, J. H., & Churchwell, E. 1986, *ApJ*, 303, 239
- Benaglia, P., & Cappa, C. E. 1999, *A&A*, 346, 979
- Benaglia, P., Romero, G. E., Stevens, I. R., & Torres, D. F. 2001, *A&A*, 366, 605
- Bernabeu, G., Magazzù, A., & Stalio, R. 1989, *A&A*, 226, 215
- Biegging, J. H., Abbott, D. C., & Churchwell, E. 1989, *ApJ*, 340, 518
- Cappa, C. E., & Benaglia, P. 1998, *AJ*, 116, 1906
- Chapman, J. M., Leitherer, C., Koribalski, B., Bouter, R., & Storey, M. 1999, *ApJ*, 518, 890
- Chlebowski, T., & Garmany, C. D. 1991, *ApJ*, 368, 241
- Conti, P. S., & Garmany, C. D. 1980, *ApJ*, 238, 190
- Contreras, M. E., Rodríguez, L. F., Gómez, Y., & Velázquez, A. 1996, *ApJ*, 469, 329
- Contreras, M. E., Rodríguez, L. F., Tapia, M., et al. 1997, *ApJ*, 488, L153
- Cruz-González, C., Recillas-Cruz, E., Costero, R., Peimbert, M., & Torres-Peimbert, S. 1974, *Rev. Mex. Astron. Astrofis.*, 1, 211
- Dougherty, S. M., & Williams, P. M. 2000, *MNRAS*, 319, 1005
- Dougherty, S. M., Williams, P. M., & Pollaco, D. L. 2000, *MNRAS*, 316, 143
- Drechsel, H., Rahe, J., Kondo, Y., & McCluskey, G. E. 1980, *A&A*, 83, 363
- Drilling, J. S. 1991, *ApJS*, 76, 1033

- Eichler, D., & Usov, V. 1993, *ApJ*, 402, 271
- Felli, M., Persi, P., Roth, M., et al. 1990, *A&A*, 232, 477
- Garmany, C. D., Conti, P. S., & Massey, P. 1980, *ApJ*, 242, 1063
- Garmany, C. D., Conti, P. S., & Chiosi, C. 1982, *ApJ*, 263, 777
- Garrison, R. F., Hiltner, W. A., & Schild, R. E. 1977, *ApJS*, 35, 111
- Gies, D. R. 1987, *ApJS*, 64, 545
- Howarth, I. D., Siebert, K. W., Hussain, G. A. J., & Prinja, R. K. 1997, *MNRAS*, 284, 265
- Hutchings, J. B. 1976, *ApJ*, 203, 438
- Hutchings, J. B. 1977, *PASP*, 89, 668
- Hutchings, J. B., & van Rudloff, I. R. 1980, *ApJ*, 238, 909
- Johnson, H. 1973, *PASP*, 85, 586
- Kudritzki, R.-P., & Puls, J. 2000, *ARA&A*, 38, 613
- Lamers, H. J. G. L. M., & Leitherer, C. 1993, *ApJ*, 412, 771
- Lamers, H. J. G. L. M., Snow, T. P., & Lindholm, D. M. 1995, *ApJ*, 455, 269
- Leitherer, C., Chapman, J. M., & Koribalski, B. 1995, *ApJ*, 450, 289
- Leitherer, C., Chapman, J. M., & Koribalski, B. 1997, *ApJ*, 481, 898
- Levato, H., Morrell, N., García, B., & Malaroda, S. 1988, *ApJS*, 68, 319
- Lindroos, K. P. 1985, *A&AS*, 60, 183
- Lozinskaya, T. A. 1982, *Ap&SS*, 87, 313
- Maeder, A. 1990, in *IAU Symp. 145, Evolution of stars: The photospheric abundance connection*, ed. G. Michaud, & A. Tutukov (Kluwer Academic Publishers), 221
- Neckel, T. 1984, *A&A*, 137, 58
- Panagia, N., & Felli, M. 1975, *A&A*, 39, 1
- Prinja, R. K., & Howarth, I. D. 1986, *ApJS*, 61, 357
- Prinja, R. K., Barlow, M. J., & Howarth, I. D. 1990, *ApJ*, 361, 607
- Puls, J., Kudritzki, R.-P., Herrero, A., et al. 1996, *A&A*, 305, 171
- Romero, G. E., Benaglia, P., & Torres, D. F. 1999, *A&A*, 348, 868
- Schmidt-Kaler, Th. 1982, in *Landolt-Börnstein, Numerical Data and Functional Relationships in Science and Technology*, ed. K. Schaifers, & H. H. Voigt (Springer, Berlin), vol. VI/2b
- Scuderi, S., Panagia, N., Stanghellini, C., Trigilio, C., & Umana, G. 1998, *A&A*, 332, 251
- Stickland, D. J. 1989, *Observatory*, 109, 74
- Thaller, M. L. 1997, *ApJ*, 487, 380
- Vacca, W. D., Garmany, C. D., & Schull, J. M. 1996, *ApJ*, 460, 914
- Vijapurkar, J., & Drilling, J. S. 1993, *A&AS*, 89, 293
- Vink, J. S., de Koter, A., & Lamers, H. J. G. L. M. 2000, *A&A*, 362, 295
- Walborn, N. 1972a, *AJ*, 77, 312
- Walborn, N. 1972b, *ApJ*, 176, L119
- Walborn, N. 1973, *AJ*, 78, 1067
- Waldron, W. L., Corcoran, M. F., Drake, S. A., & Smale, A. P. 1998, *ApJS*, 118, 217
- White, R. L. 1985, *ApJ*, 289, 698
- Wiggs, M. S., & Gies, D. R. 1993, *ApJ*, 407, 252
- Wright, A. E., & Barlow, M. J. 1975, *MNRAS*, 170, 41